Science Bulletin 68 (2023) 2164–2169

Contents lists available at ScienceDirect

Science Bulletin

journal homepage: www.elsevier.com/locate/scib

Article

Sound non-reciprocity based on synthetic magnetism

Zhaoxian Chen [a,b], Zhengwei Li [a], Jingkai Weng [a], Bin Liang [a,*], Yanqing Lu [b,*], Jianchun Cheng [a,*], Andrea Alù [c,d,*]

[a] Collaborative Innovation Center of Advanced Microstructures, Key Laboratory of Modern Acoustics of Ministry of Education, Institute of Acoustics, Department of Physics, Nanjing University, Nanjing 210093, China
[b] College of Engineering and Applied Sciences, Nanjing University, Nanjing 210093, China
[c] Photonics Initiative, Advanced Science Research Center, City University of New York, New York NY 10031, USA
[d] Physics Program, Graduate Center, City University of New York, New York NY 10016, USA

ARTICLE INFO

Article history:
Received 28 February 2023
Received in revised form 22 April 2023
Accepted 17 July 2023
Available online 9 August 2023

Keywords:
Synthetic magnetism
Sound non-reciprocity
Time modulation
Dynamic coupling

ABSTRACT

Synthetic magnetism has been recently realized using spatiotemporal modulation patterns, producing non-reciprocal steering of charge-neutral particles such as photons and phonons. Here, we design and experimentally demonstrate a non-reciprocal acoustic system composed of three compact cavities interlinked with both dynamic and static couplings, in which phase-correlated modulations induce a synthetic magnetic flux that breaks time-reversal symmetry. Within the rotating wave approximation, the transport properties of the system are controlled to efficiently realize large non-reciprocal acoustic transport. By optimizing the coupling strengths and modulation phases, we achieve frequency-preserved unidirectional transport with 45-dB isolation ratio and 0.85 forward transmission. Our results open to the realization of acoustic non-reciprocal technologies with high efficiency and large isolation, and offer a route towards Floquet topological insulators for sound.

1. Introduction

In conventional linear and time-independent media, wave propagation is usually reciprocal and the scattering matrix of the system is symmetric [1,2]. Breaking reciprocity is of fundamental interest for wave physics and it may enhance existing technologies built on the assumption of reciprocal wave transmission. In particular, the intrinsic lack of strong magneto-acoustic effects prohibits non-reciprocal steering of acoustic waves using magnetic materials as commonly done in the electromagnetic domain. Non-reciprocal steering for sound has been realized using asymmetric nonlinearities [3–5], then followed by using biased media flow [6,7]. However, non-reciprocity with nonlinear media is amplitude-dependent, and the output suffers from phase noise and frequency distortion. The introduction of directional media flow provides the possibility of breaking time-reversal symmetry without affecting the signal frequency, however, such mechanisms typically introduce undesired noise at high flow speed and may be impractical in integrated acoustic technologies.

Recently, time modulation has attracted rapidly-growing attention as an effective alternative to realize non-reciprocity for photonics [8,9] and acoustics [1,10]. A synthetic momentum of the medium can be imparted by modulating it in time and space with a travelling wave-like modulation scheme, realizing asymmetric indirect mode transitions that break reciprocity [11–13]. Despite considerable efforts dedicated to implementing such modulation with airborne sound [14–16] and elastic waves [17–20], the achieved isolation ratio has so far been limited [21,22]. On the other hand, when the medium is modulated uniformly, direct mode transitions cannot directly break reciprocity, but instead, they can introduce an effective gauge field [23–25]. By combining two or more of such mode transitions, we can then realize non-reciprocity based on the introduction of a synthetic magnetic field [26–29]. However, due to the lack of efficient modulation techniques, acoustic non-reciprocity based on synthetic magnetism has been rarely reported [30,31]. To date, it still remains challenging to realize acoustic non-reciprocity with high forward transmission, large isolation and avoiding frequency conversion.

In this work, we propose to overcome these limitations by relying on synthetic magnetism imparted by time modulation and demonstrate both theoretically and experimentally an implementation by designing an acoustic cavity system with large and efficient unidirectional transmission features. A novel mechanism to

* Corresponding authors.
E-mail addresses: liangbin@nju.edu.cn (B. Liang), yqlu@nju.edu.cn (Y. Lu), jccheng@nju.edu.cn (J. Cheng), aalu@gc.cuny.edu (A. Alù).

https://doi.org/10.1016/j.scib.2023.08.013
2095-9273/

modulate the acoustic coupling both in sign and strength is introduced to achieve this goal. By controlling the coupling phases, we are able to synthesize an effective magnetic bias for sound that breaks time-reversal symmetry and realizes an efficient and frequency-preserving non-reciprocal acoustic system. The measured isolation ratio is as high as 45 dB, and the forward transmission is 0.85, which can be further improved by optimizing the design. Without relying on airflow or mechanical motion, our non-reciprocal system is stable, robust, and compact, and it can serve as an excellent platform for topological and non-Hermitian acoustics.

2. Theory and results

2.1. Synthetic magnetism with time modulation

The proposed non-reciprocal device is schematically shown in Fig. 1 and it consists of three cavities labeled with A, B, and C. The cavities A and C are identical in size and have the same resonance frequency, namely $\omega_C = \omega_A$. Cavity B is detuned by making it smaller, so that it supports a larger resonance frequency ω_B. Between A and C, we introduce a static coupling k_{AC} that introduces a reciprocal transfer phase φ_{static}. In addition, A and C are interlinked through B with a time-varying coupling coefficient $k_{AB}(t) = \Delta k\cos(\Omega t + \varphi_1)$ and $k_{BC}(t) = \Delta k\cos(\Omega t + \varphi_2)$, where Δk is the coupling amplitude, $\Omega = \omega_B - \omega_A$ is the modulation frequency, and φ_1 and φ_2 are the initial phases. We select the modulation frequency to be the frequency difference between the detuned cavities, realizing efficient frequency conversion and coupling. We define the forward (backward) direction as from A (C) to C (A). To clearly explain the phenomena underlying non-reciprocal transmission, we first set $k_{AC} = 0$. For the forward transmission, the operating frequency of the source is $\omega = \omega_A$, enabling efficient excitation of the resonance in cavity A. According to temporal Floquet theory [32], the generated +1 order harmonic with phase φ_1 is strictly at ω_B and can resonantly excite B. Other orders of harmonics are far from the cavity's resonance and are negligible. Then the sound wave in B transfers to C and goes back to ω_A with another phase $-\varphi_2$. As a result, the dynamic modulation phases induce an effective magnetic vector potential $\vec{A}$, and the phase for the forward transmission (A to C) is $\varphi^f_{dynamic} = \int_A^B \vec{A}\cdot d\vec{l} + \int_B^C \vec{A}\cdot d\vec{l} = \varphi_1 - \varphi_2$. However, for the backward transmission (C to A), the phase flips sign, namely $\varphi^b_{dynamic} = -\varphi^f_{dynamic}$. Similar to the Aharonov-Bohm effect for electrons [33], here the dynamic modulations work as the synthetic magnetism to break the time-reversal symmetry, rendering the transmission phase non-reciprocal. When both static and dynamic couplings are considered and the phases satisfy $\varphi^f_{dynamic} \approx \varphi_{static} \approx \pi/2$, there is constructive interference between the two transmitting waves, implying an efficient transfer from A to C. In contrast, when the direction is reversed, $\varphi^b_{dynamic} \approx -\varphi_{static}$, and the signal cannotpropagate because of destructive interference. As a consequence, we realize frequency-preserving non-reciprocal transmission with large forward transmission and isolation. This mechanism for non-reciprocity is different from, and more generally applicable than synthetic angular momentum bias realized by modulating in time different cavities on site with specific phase patterns [34–36]. In the following, we experimentally verify our proposed scheme and demonstrate non-reciprocal transmission of airborne sound in a practical system.

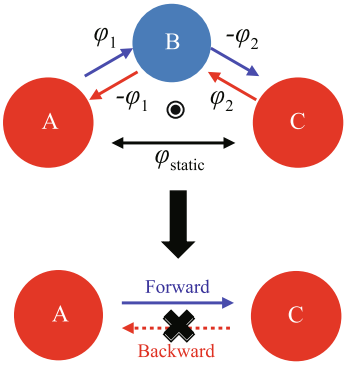

Fig. 1. (Color online) Non-reciprocal wave system with synthetic magnetism. The resonance frequency of the cavities is $\omega_C = \omega_A$ and $\omega_B = \Omega + \omega_A$. The static coupling between A and C contributes a reciprocal transmission phase φ_{static}. In addition, there are dynamic couplings between A and B (B and C), $k_{AB}(t) = \Delta k\cos(\Omega t + \varphi_1)$ and $k_{BC}(t) = \Delta k\cos(\Omega t + \varphi_2)$. These elements couple the resonant fields to adjacent Floquet harmonics, and the phases induce a synthetic magnetic flux (black point circle) that breaks time-reversal symmetry. Combined static and dynamic couplings induce non-reciprocal power transmission and isolation between A and C.

2.2. Tunable coupling with electric control

We used an in-house-designed electric setup to realize tunable coupling among the acoustic cavities. Fig. 2a shows the photo of the fabricated metallic acoustic cavities and the active circuit consisting of loudspeakers (for output), microphones (for input), and a signal amplifier (with direct current power supply). Sound is detected at resonator A (B) by the microphones, and then coupled to resonator B (A) by loudspeakers after amplification. In this way, the electric coupling between the two cavities can be modulated fast and precisely. We make sure that the realized coupling is linear and bi-directional to avoid spurious non-reciprocal effects

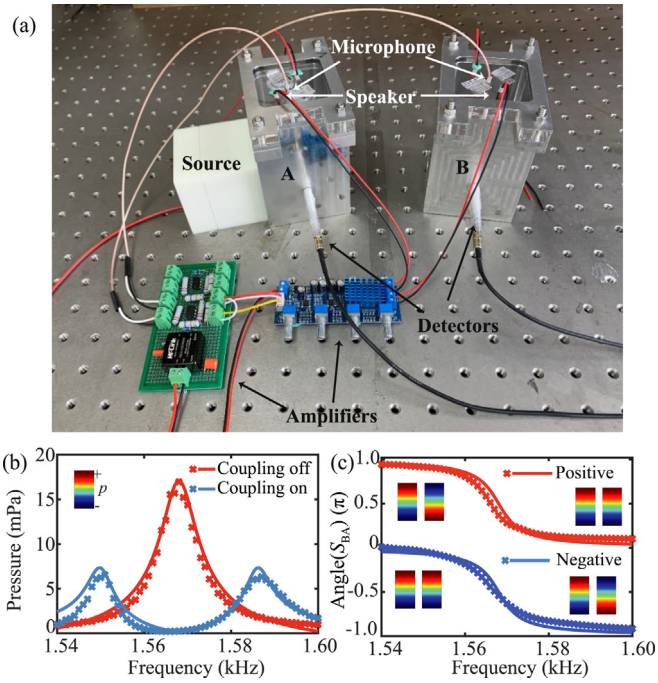

Fig. 2. (Color online) Tunable coupling with electric control. (a) Experimental design to realize the coupling between two conoid acoustic cavities (labeled A and B). The microphones detect the sound in A (B), and then couple it to B (A) through the loudspeakers after amplification. A sound source is used to excite the system, and other two microphones are inserted into the cavity to extract the pressure information. (b) Measured (crosses) and fitted (solid lines) pressure in A with (blue) and without (red) coupling. (c) The transmission phase angle (S_{BA}) for positive (red) and negative (blue) coupling.

that may come from the microphone-to-loudspeaker connection. The cavities are cuboids in shape, and their heights are adjustable to tune the resonant frequencies (see Supplementary materials S1 online for details).

In this work, we focus on the first-order resonant mode with a dipole-like mode profile (inset in Fig. 2b), which is beneficial to design different coupling effects. By fitting the excitation spectrum of a single cavity, as shown in Fig. 2b, we get the resonance frequency $\frac{\omega_A}{2\pi} = 1568$ Hz and intrinsic loss rate $\frac{\gamma}{2\pi} = 4.5$ Hz. The coupling between two such cavities, which is realized through the designed electric setup, is characterized by the splitting of the spectrum into two peaks. This coupling can be modeled with a static Hamiltonian $\boldsymbol{H} = [\omega_A + i\gamma, k; k, \omega_A + i\gamma]$, where k is the coupling coefficient [37]. According to coupling mode theory, the amplitude k is determined by the distance of the two peaks. Here $|k|$ = 17 Hz, whose sign depends on the phase difference between the two cavities, as shown by the simulated field profiles in Fig. 2c. We define the ratio of pressures between B and A as the transmission $S_{BA}(\omega) = k/(\omega - \omega_A - i\gamma)$ (see Supplementary materials S2 online for details). When the microphones and the loudspeakers are connected in-phase, as shown by the red curves, the two cavities are in-phase (out-of-phase) for the higher (lower) frequency range, indicating a positive coupling effect. However, by simply inverting the connections between microphones and loudspeakers, negative coupling is realized due to the flipping of the field parities (see the blue curves and the insets). As a result, our electric setups offer the possibility of designing and tuning the coupling in a way unattainable with existing methods (see Supplementary materials S3 online for comparison) [38–42].

2.3. Frequency conversion with dynamic coupling

Next, we design the time-periodic coupling between two cavities, as schematically illustrated in Fig. 3a. Firstly, we decrease B's height by 4 mm to increase its resonant frequency to $\frac{\omega_B}{2\pi} = 1623$ Hz. Two double-pole, double-throw (DPDT) relays are remolded and inserted between the amplifier and the loudspeakers. A square wave voltage signal with $\frac{\Omega}{2\pi} = \frac{\omega_B - \omega_A}{2\pi} = 55$ Hz is applied to the relays such that the circuit condition changes between

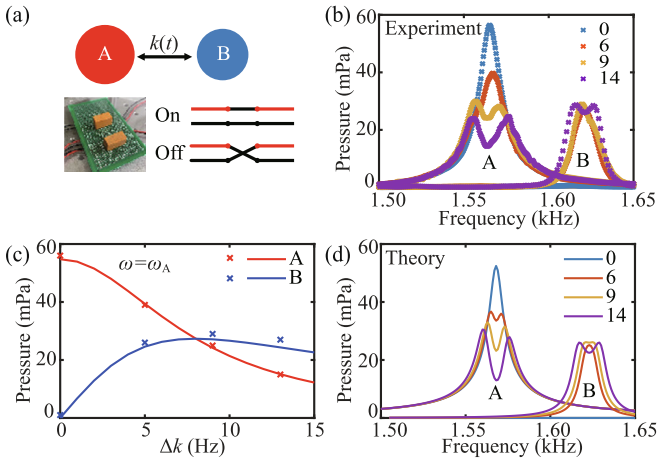

Fig. 3. (Color online) Frequency conversion with dynamic coupling. (a) The upper panel shows the dynamic coupling between two different cavities. The lower panel shows the photograph of the DPDT relays and the on (off) circuit conditions with (without) the controlling voltage signals. (b) Measured pressures in A and B with different coupling strengths Δk. (c) Calculated pressures (solid curves) in A (red) and B (blue) fit the measured pressure (crosses) for $\omega = \omega_A$. (d) Calculated pressures in A and B for different Δk.

in-phase and out-of-phase repeatedly, resulting in a periodic switching between positive and negative coupling. The two cavities only support their first-order resonant modes around 1600 Hz. As a result, the frequency conversion process is limited to the first-order Floquet harmonics. It is reasonable to treat the dynamic coupling as $k(t) = \Delta k \cos(\Omega t + \varphi)$, where Δk is the effective coupling amplitude and φ is the initial phase. Therefore, the Hamiltonian of this time-dependent system is written as

$$H(t, \varphi) = \begin{bmatrix} \omega_A + i\gamma & \Delta k \cos(\Omega t + \varphi) \\ \Delta k \cos(\Omega t + \varphi) & \omega_B + i\gamma \end{bmatrix}. \quad (1)$$

When A is excited, we simultaneously measure the pressure in these two cavities. The experimental results in Fig. 3b show that the acoustic waves are transmitted from A to B with a frequency increase of Ω. To quantitatively evaluate the dynamic coupling effect, temporal coupled model theory (CMT) is employed, for the state function of the system $|\Psi(t)\rangle = [a(t), b(t)]^T$. According to Floquet theory, the signals in the two cavities can be expanded as $a, b(t) = \sum_n a_n, b_n e^{i(\omega + n\Omega)t}$, where a_n and b_n are the time-independent wave amplitude of the n-th order Floquet harmonic, and ω is the excitation frequency. Then the temporal evolution of the system can be described with a Schrödinger-type differential equation:

$$-i\frac{d}{dt}|\Psi(t)\rangle = \boldsymbol{H}(t)|\Psi(t)\rangle + s(t), \quad (2)$$

where $s(t) = [P_{in} e^{i\omega t}, 0]^T$ is the excitation. After some algebra, the coupled-mode equations can be expressed as [43,44]

$$(\omega + n\Omega - \omega_A - i\gamma)a_n - \frac{\Delta k e^{i\varphi} b_{n+1}}{2} - \frac{\Delta k e^{-i\varphi} b_{n-1}}{2} = P_{in}\delta_{n0}, \quad (3a)$$

$$(\omega + n\Omega - \omega_B - i\gamma)b_n - \Delta k e^{i\varphi} a_{n+1}/2 - \Delta k e^{-i\varphi} a_{n-1}/2 = 0, \quad (3b)$$

where δ_{n0} is the Kronecker delta function. From these equations, we see that the cavities are coupled through adjacent harmonics. By truncating the system to finite Floquet harmonics, we solve these coupled equations and obtain the pressure in the two cavities with different coupling strengths. For the case $\omega = \omega_A$, as shown in Fig. 3c, there is an optimal Δk that couples the acoustic wave from A to B, because of the trade-off between input coupling and harmonic conversion. By fitting the measured pressure in A, we can estimate the Δk values. Comparison between Fig. 3b and d suggests that the temporal CMT well explains the dynamic coupling effect.

2.4. Sound isolation with outstanding performance

Next, another cavity C is added to form a three-cavity system with non-reciprocal transmission features. As schematically shown in Fig. 1, now the total coupling is composed of a static coupling k_{AC} and two dynamic couplings with initial phase φ_1 and φ_2 respectively. For this system, the state function is $|\Psi(t)\rangle = [a(t), b(t), c(t)]^T$ and the temporal Hamiltonian is

$$H(t, \varphi_1, \varphi_2) = \begin{bmatrix} \omega_A + i\gamma & \Delta k \cos(\Omega t + \varphi_1) & k_{AC} \\ \Delta k \cos(\Omega t + \varphi_1) & \omega_B + i\gamma & \Delta k \cos(\Omega t + \varphi_2) \\ k_{AC} & \Delta k \cos(\Omega t + \varphi_2) & \omega_C + i\gamma \end{bmatrix}. \quad (4)$$

Since the modulation frequency is the difference between cavities, we can perform a transformation to simplify this system: we define a new state function $|\Phi(t)\rangle = M^{-1}|\Psi(t)\rangle$, where

$$M^{-1} = \begin{bmatrix} 1 & 0 & 0 \\ 0 & e^{-i\Omega t} & 0 \\ 0 & 0 & 1 \end{bmatrix}. \quad (5)$$

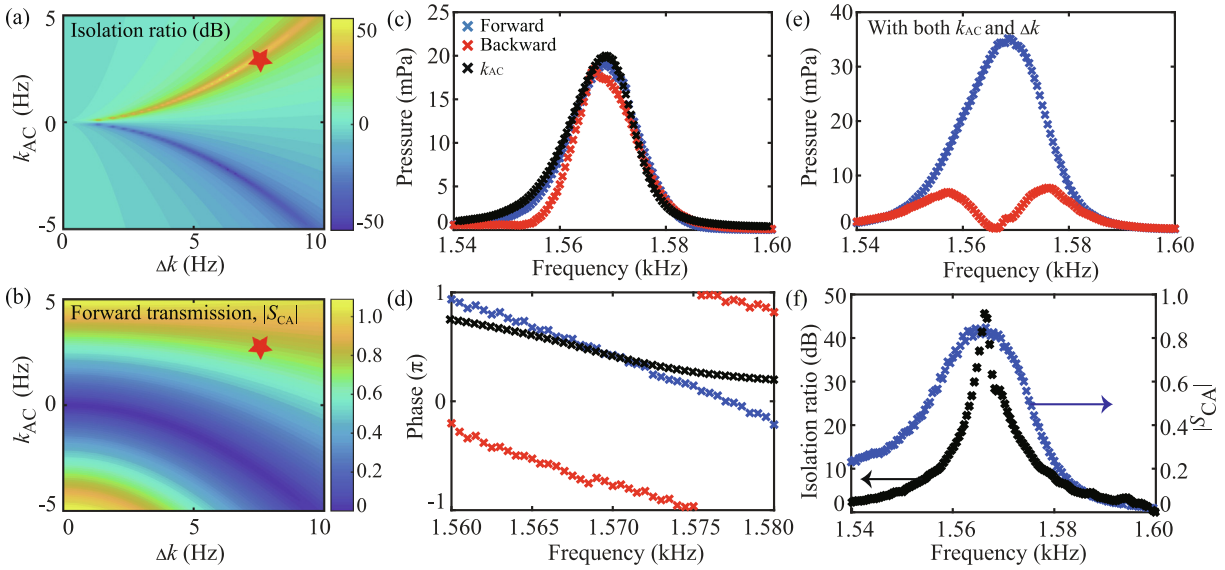

Fig. 4. (Color online) Non-reciprocal sound power transmission. Calculated isolation ratio (a) and forward transmission (b) for $\omega = \omega_A$ and $\Delta\varphi = \pi/2$. The red stars denote the experimental case with $\frac{\Delta k}{2\pi} = 7.5$ Hz and $\frac{k_{AC}}{2\pi} = 3$ Hz. Measured transmitting pressures (c) and transmitting phases (d) with either Δk or k_{AC}. (e) Measured transmitting pressures with both Δk and k_{AC}. (f) Measured isolation ratio and forward transmission.

Using the rotating wave approximation [23], we get a simplified wave function:

$$-\mathrm{i}\frac{\mathrm{d}}{\mathrm{d}t}|\Phi(t)\rangle = \begin{bmatrix} \omega_A + \mathrm{i}\gamma & \Delta k \mathrm{e}^{-\mathrm{i}\varphi_1}/2 & k_{AC} \\ \Delta k \mathrm{e}^{\mathrm{i}\varphi_1}/2 & \omega_B + \mathrm{i}\gamma & \Delta k \mathrm{e}^{\mathrm{i}\varphi_2}/2 \\ k_{AC} & \Delta k \mathrm{e}^{-\mathrm{i}\varphi_2}/2 & \omega_C + \mathrm{i}\gamma \end{bmatrix} |\Phi(t)\rangle. \tag{6}$$

Solving these coupled equations, we obtain the transmission coefficients (see Supplementary materials S4 online for detailed derivations):

$$S_{CA}(\omega) = \frac{\frac{\mathrm{e}^{\mathrm{i}\Delta\varphi}\Delta k^2}{4} + (\omega - \omega_A - \mathrm{i}\gamma)k_{AC}}{(\omega - \omega_A - \mathrm{i}\gamma)^2 - \frac{\Delta k^2}{4}}, \tag{7a}$$

$$S_{AC}(\omega) = \frac{\frac{\mathrm{e}^{-\mathrm{i}\Delta\varphi}\Delta k^2}{4} + (\omega - \omega_A - \mathrm{i}\gamma)k_{AC}}{(\omega - \omega_A - \mathrm{i}\gamma)^2 - \frac{\Delta k^2}{4}}, \tag{7b}$$

where $\Delta\varphi = \varphi_1 - \varphi_2$. Clearly, when $\Delta\varphi = \pi/2$ and $k_{AC} = \Delta k^2/4\gamma$, we obtain $S_{AC}(\omega_A) = 0$, which implies that the transmitted waves originated from the static and dynamic coupling effects destructively interfere in the backward direction and the transmission from C to A is suppressed. In contrast, the forward transmission is enhanced, since the two transmitting waves are in phase. In Fig. 4a, b, we plot the isolation ratio $20\log|S_{CA}(\omega_A)/S_{AC}(\omega_A)|$ and the forward transmission $|S_{CA}(\omega_A)|$ with $\Delta\varphi = \pi/2$. By optimizing the strength of the couplings, we can get efficient and unidirectional power transmission.

As an experimental demonstration (red stars in Fig. 4a, b), we present the measured amplitudes and phases of the transmitted waves for different coupling conditions, in good agreement with our theoretical predictions (see Supplementary materials S5 online for the comparison). When there is only Δk, as shown in Fig. 4c, d, the transmission magnitudes are almost identical for both forward (blue) and backward (red) directions. However, their phases have a difference of π, which is attributed to time-reversal symmetry breaking due to the applied synthetic magnetic field. We note here that the transmission is only non-reciprocal in terms of transmission phase, realizing an acoustic gyrator. On the other hand, when only k_{AC} exists, the transmission amplitudes and phases are identical for both directions (only one direction is shown for simplicity), as expected. When both Δk and k_{AC} are present, we realize the expected non-reciprocal power transmission, as seen by the enhanced forward transmission (blue) and nearly-blocked backward transmission (red) near ω_A, as shown in Fig. 4e. Due to the resonant feature of the cavities, the maximum isolation ratio is achieved around the resonant frequency of the input cavity. As shown in Fig. 4f, the isolation ratio reaches 45 dB, and the forward transmission is high up to 0.85. More importantly, it is noteworthy that our mechanism allows further improving the forward transmission by optimizing the coupling strength. As a result, we have realized acoustic non-reciprocity based on temporal modulation of the coupling between cavities, making an important step towards the realization of integrated and compact acoustic isolators. For the cases with $\Delta\varphi = \pi$ or $\Delta\varphi = 0$, the transmission phases for both directions are identical, thus there is no isolation effects (see Supplementary materials S6 and S7 online for more results).

3. Conclusion

To conclude, we have demonstrated a frequency-preserving non-reciprocal acoustic system based on a mechanism that breaks time-reversal symmetry by utilizing modulation phases to induce a synthetic magnetic field. The measured performance is in good agreement with our theoretical predictions, demonstrating that the isolation reaches 45 dB, while the forward transmission is as high as 0.85. Due to the cascaded conversion processes in the system, the transmitted wave has the original frequency, in stark contrast to previous works in which the transmitting signals are mixed with other harmonics when spatial–temporal modulations or nonlinear media are utilized. The proposed strategy for time modulation strategy bears the advantages in terms of speed, efficiency, and flexibility, which opens up new avenues for non-reciprocal sound devices and Floquet topological insulators with real time modulation [23,35], and may also inspire new research for non-Hermitian acoustics [45–47].

Conflict of interest

The authors declare that they have no conflict of interest.

Acknowledgments

This work was supported by the National Key Research and Development Program of China (2017YFA0303700, 2022YFA1404400, and 2022YFA1405000), the Natural Science Foundation of Jiangsu Province (BK20212004), the National Natural Science Foundation of China (11634006, 11374157, and 81127901), a project funded by the Priority Academic Program Development of Jiangsu Higher Education Institutions, the High-Performance Computing Center of Collaborative Innovation Center of Advanced Microstructures, the Air Force Office of Scientific Research, and the Simons Foundation. Zhaoxian Chen acknowledges support from the China Postdoctoral Science Foundation (2023M731609).

Author contributions

Zhaoxian Chen, Bin Liang, and Andrea Alù conceived the idea and designed the experiment. Zhaoxian Chen, Zhengwei Li, and Jingkai Weng prepared the samples and performed the experiment. Zhaoxian Chen conducted theoretical calculations. All the authors contributed to the writing of the paper. Bin Liang, Yanqing Lu, Jianchun Cheng, and Andrea Alù supervised the entire study.

Appendix A. Supplementary materials

Supplementary materials to this article can be found online at https://doi.org/10.1016/j.scib.2023.08.013.

References

[1] Nassar H, Yousefzadeh B, Fleury R, et al. Nonreciprocity in acoustic and elastic materials. Nat Rev Mater 2020;5:667–85.
[2] Caloz C, Alù A, Tretyakov S, et al. Electromagnetic nonreciprocity. Phys Rev Appl 2018;10:047001.
[3] Liang B, Yuan B, Cheng JC. Acoustic diode: rectification of acoustic energy flux in one-dimensional systems. Phys Rev Lett 2009;103:104301.
[4] Liang B, Guo XS, Tu J, et al. An acoustic rectifier. Nat Mater 2010;9:989–92.
[5] Boechler N, Theocharis G, Daraio C. Bifurcation-based acoustic switching and rectification. Nat Mater 2011;10:665–8.
[6] Fleury R, Sounas DL, Sieck CF, et al. Sound isolation and giant linear nonreciprocity in a compact acoustic circulator. Science 2014;343:516.
[7] Ding Y, Peng Y, Zhu Y, et al. Experimental demonstration of acoustic chern insulators. Phys Rev Lett 2019;122:014302.
[8] Sounas DL, Alù A. Non-reciprocal photonics based on time modulation. Nat Photonics 2017;11:774–83.
[9] Williamson IAD, Minkov M, Dutt A, et al. Integrated nonreciprocal photonic devices with dynamic modulation. Proc IEEE 2020;108:1759–84.
[10] Rasmussen C, Quan L, Alù A. Acoustic nonreciprocity. J Appl Phys 2021;129:210903.
[11] Yu Z, Fan S. Complete optical isolation created by indirect interband photonic transitions. Nat Photonics 2009;3:91–4.
[12] Lira H, Yu Z, Fan S, et al. Electrically driven nonreciprocity induced by interband photonic transition on a silicon chip. Phys Rev Lett 2012;109:033901.
[13] Guo X, Ding Y, Duan Y, et al. Nonreciprocal metasurface with space-time phase modulation. Light Sci Appl 2019;8:123.
[14] Zanjani MB, Davoyan AR, Mahmoud AM, et al. One-way phonon isolation in acoustic waveguides. Appl Phys Lett 2014;104:081905.
[15] Li J, Shen C, Zhu X, et al. Nonreciprocal sound propagation in space-time modulated media. Phys Rev B 2019;99:144311.
[16] Wen X, Zhu X, Wu HW, et al. Realizing spatiotemporal effective media for acoustic metamaterials. Phys Rev B 2021;104:L060304.
[17] Trainiti G, Ruzzene M. Non-reciprocal elastic wave propagation in spatiotemporal periodic structures. New J Phys 2016;18:083047.
[18] Nassar H, Chen H, Norris AN, et al. Non-reciprocal wave propagation in modulated elastic metamaterials. Proc R Soc A Math Phys Eng Sci 2017;473:20170188.
[19] Wang Y, Yousefzadeh B, Chen H, et al. Observation of nonreciprocal wave propagation in a dynamic phononic lattice. Phys Rev Lett 2018;121:194301.
[20] Chen Y, Li X, Nassar H, et al. Nonreciprocal wave propagation in a continuum-based metamaterial with space-time modulated resonators. Phys Rev Appl 2019;11:064052.
[21] Xu X, Wu Q, Chen H, et al. Physical observation of a robust acoustic pumping in waveguides with dynamic boundary. Phys Rev Lett 2020;125:253901.
[22] Chen Z, Peng Y, Li H, et al. Efficient nonreciprocal mode transitions in spatiotemporally modulated acoustic metamaterials. Sci Adv 2021;7:eabj1198.
[23] Fang K, Yu Z, Fan S. Realizing effective magnetic field for photons by controlling the phase of dynamic modulation. Nat Photonics 2012;6:782–7.
[24] Fang K, Yu Z, Fan S. Photonic Aharonov-Bohm effect based on dynamic modulation. Phys Rev Lett 2012;108:153901.
[25] Yuan L, Lin Q, Xiao M, et al. Synthetic dimension in photonics. Optica 2018;5:1396–405.
[26] Li E, Eggleton BJ, Fang K, et al. Photonic Aharonov-Bohm effect in photon–phonon interactions. Nat Commun 2014;5:3225.
[27] Tzuang LD, Fang K, Nussenzveig P, et al. Non-reciprocal phase shift induced by an effective magnetic flux for light. Nat Photonics 2014;8:701–5.
[28] Fang K, Luo J, Metelmann A, et al. Generalized non-reciprocity in an optomechanical circuit via synthetic magnetism and reservoir engineering. Nat Phys 2017;13:465–71.
[29] Peterson CW, Benalcazar WA, Lin M, et al. Strong nonreciprocity in modulated resonator chains through synthetic electric and magnetic fields. Phys Rev Lett 2019;123:063901.
[30] Dai DD, Zhu XF. An effective gauge potential for nonreciprocal acoustics. EPL 2013;102:14001.
[31] Qin C, Peng Y, Li Y, et al. Spectrum manipulation for sound with effective gauge fields in cascading temporally modulated waveguides. Phys Rev Appl 2019;11:064012.
[32] Shirley JH. Solution of the Schrödinger equation with a Hamiltonian periodic in time. Phys Rev 1965;138:B979–87.
[33] Aharonov Y, Bohm D. Significance of electromagnetic potentials in the quantum theory. Phys Rev 1959;115:485–91.
[34] Estep NA, Sounas DL, Soric J, et al. Magnetic-free non-reciprocity and isolation based on parametrically modulated coupled-resonator loops. Nat Phys 2014;10:923–7.
[35] Fleury R, Khanikaev AB, Alu A. Floquet topological insulators for sound. Nat Commun 2016;7:11744.
[36] Fleury R, Sounas DL, Alù A. Subwavelength ultrasonic circulator based on spatiotemporal modulation. Phys Rev B 2015;91:174306.
[37] Ding K, Ma G, Xiao M, et al. Emergence, coalescence, and topological properties of multiple exceptional points and their experimental realization. Phys Rev X 2016;6:021007.
[38] Chen Z, Chen Z, Li Z, et al. Topological pumping in acoustic waveguide arrays with hopping modulation. New J Phys 2021;24:013004.
[39] Xue H, Ge Y, Sun HX, et al. Observation of an acoustic octupole topological insulator. Nat Commun 2020;11:2442.
[40] Qi Y, Qiu C, Xiao M, et al. Acoustic realization of quadrupole topological insulators. Phys Rev Lett 2020;124:206601.
[41] Ni X, Li M, Weiner M, et al. Demonstration of a quantized acoustic octupole topological insulator. Nat Commun 2020;11:2108.
[42] Zhang L, Yang Y, Ge Y, et al. Acoustic non-hermitian skin effect from twisted winding topology. Nat Commun 2021;12:6297.
[43] Koutserimpas TT, Fleury R. Nonreciprocal gain in non-hermitian time-floquet systems. Phys Rev Lett 2018;120:087401.
[44] Shen C, Zhu X, Li J, et al. Nonreciprocal acoustic transmission in space-time modulated coupled resonators. Phys Rev B 2019;100:054302.
[45] Ghatak A, Brandenbourger M, van Wezel J, et al. Observation of non-Hermitian topology and its bulk–edge correspondence in an active mechanical metamaterial. Proc Natl Acad Sci USA 2020;117:29561–8.
[46] Hu B, Zhang Z, Zhang H, et al. Non-hermitian topological whispering gallery. Nature 2021;597:655–9.
[47] Wang W, Wang X, Ma G. Non-hermitian morphing of topological modes. Nature 2022;608:50–5.

Zhaoxian Chen received his bachelor's and Ph.D. degrees from Nanjing University in 2012 and 2022, respectively. Now he is a postdoctoral fellow at Nanjing University. His research interest mainly focuses on time-varying phononic and photonic systems.

Bin Liang received his bachelor's and Ph.D. degrees from Nanjing University in 2002 and 2007, respectively. Now he is the director of Key Laboratory of Modern Acoustics of Ministry of Education and a full professor at the Department of Physics, Nanjing University. His research interest mainly focuses on acoustic metamaterials/metasurfaces and their applications.

Yanqing Lu received his Ph.D. degree from Nanjing University in 1996. He is the vice president of Nanjing University and a professor at the College of Engineering and Applied Sciences, Nanjing University. His research interest mainly focuses on metamaterials for photonics and phononics.

Jianchun Cheng received his Ph.D. degree from Nanjing University in 1992 and started to teach at the university after graduation. He worked at Brown University and Georgia Institute of Technology as a visiting scholar in 1996 and 2000, respectively. His research interest includes acoustic physics and acoustic metamaterials.

Andrea Alù received the Laurea, M.S. and Ph.D. degrees from the University of Roma Tre, Italy, respectively in 2001, 2003, and 2007. In 2009 he joined the faculty of the University of Texas at Austin. In 2018 he moved to the City University of New York (CUNY), where he founded the Photonics Initiative at the CUNY Advanced Science Research Center (ASRC). His research interest includes metamaterials and plasmonics, electromangetics, optics and photonics, scattering, cloaking and transparency, nanocircuits and nanostructures modeling, miniaturized antennas and nanoantennas, radio-frequency antennas and circuits, acoustic and mechanical devices and metamaterials.